Prolonged irradiation of enhanced cyan fluorescent protein or Cerulean can invalidate Förster resonance energy transfer measurements

Birgit Hoffmann
Thomas Zimmer
Universitätsklinikum Jena
Institut für Physiologie II
Kollegiengasse 9
07740 Jena, Germany

Nikolaj Klöcker
Albert-Ludwigs-Universität Freiburg
Institut für Physiologie
79104 Freiburg, Germany

Laimonas Kelbauskas*
Universitätsklinikum Jena
Institut für Physiologie II
Kollegiengasse 9
07740 Jena, Germany

Karsten König
Saarland University
Faculty of Physics and Mechatronics
66123 Saarbrücken, Germany

Klaus Benndorf
Christoph Biskup
Universitätsklinikum Jena
Institut für Physiologie II
Kollegiengasse 9
07740 Jena, Germany

Abstract. Since its discovery, green fluorescent protein (GFP) and its variants have proven to be a good and convenient fluorescent label for proteins: GFP and other visible fluorescent proteins (VFPs) can be fused selectively to the protein of interest by simple cloning techniques and develop fluorescence without additional cofactors. Among the steadily growing collection of VFPs, several pairs can be chosen that can serve as donor and acceptor fluorophores in Förster resonance energy transfer (FRET) experiments. Among them, the cyan fluorescent proteins (ECFP/Cerulean) and the enhanced yellow fluorescent protein (EYFP) are most commonly used. We show that ECFP and Cerulean have some disadvantages despite their common use: Upon irradiation with light intensities that are commonly used for intensity- and lifetime-based FRET measurements, both the fluorescence intensity and the fluorescence lifetime of ECFP and Cerulean decrease. This can hamper both intensity- and lifetime-based FRET measurements and emphasizes the need for control measurements to exclude these artifacts.
[DOI: 10.1117/1.2937829]

Keywords: enhanced cyan fluorescent protein; Cerulean; time-resolved spectroscopy; streak camera; Förster resonance energy transfer; fluorescence resonance energy transfer; fluorescence lifetime imaging; photobleaching; photoconversion.

Paper 07328SSR received Aug. 13, 2007; revised manuscript received Dec. 20, 2007; accepted for publication Dec. 21, 2007; published online Jul. 1, 2008.

1 Introduction

Since its discovery[1] in the jellyfish *Aequorea victoria* and the cloning of the gene,[2–4] green fluorescent protein (GFP) has proven to be a valuable tool for labeling proteins: instead of labeling the proteins directly, the genetic code of GFP or of one of its variants is fused by simple cloning techniques to the sequence of the protein of interest. Upon expression of the protein, the fluorescent tag is also expressed and develops fluorescence without additional cofactors.[5] As opposed to classical labeling techniques involving fluorescent dyes, proteins of interest can be labeled selectively in this way. Because of this and their ease of application, visible fluorescent proteins (VFPs) have been widely used to study the subcellular localization and trafficking of proteins. For the same reason, VFPs are also employed extensively in fluorescence resonance energy transfer (FRET) experiments to detect and trace protein-protein interactions in living cells. When the proteins of interest interact, donor and acceptor fluorophores are brought into close vicinity so that the donor can transmit its excitation energy to the acceptor. As a result, both the intensity and the lifetime of the donor fluorescence decrease, whereas the intensity of the acceptor emission increases.[6] This offers several approaches to determine FRET efficiency on the stage of a fluorescence microscope: One is to detect changes in the intensity of donor and acceptor emission,[7,8] the other is to measure changes in the lifetime of the donor molecule.[9,10] One important advantage of the latter approach is that fluorescence lifetimes are independent of the actual protein concentrations. Therefore, control measurements can be obtained from different cells. Moreover the fluorescence decay offers additional information that can be used to calculate the relative fractions of free and associated donor molecules.[11]

As opposed to the well-established biochemical methods, microscopic techniques that exploit FRET between VFPs are

*Current address: Arizona State University, 1001 South McAllister Ave., Tempe, AZ 85287.
Address all correspondence to Dr. Christoph Biskup, Universitätsklinikum Jena, Institut für Physiologie II, Teichgraben 8, D 07740 Jena, Germany; Tel.: +49–3641–938874; Fax: +49–3641–933202; E-mail: christoph.biskup@mti.uni-jena.de

1083-3668/2008/13(3)/031205/9/$25.00 © 2008 SPIE

able not only to *detect* but also to *track* protein-protein interactions in living cells. *When* and *where* proteins associate with each other in living cells are key questions in many biological research areas, and the preceding techniques have the power to provide answers to many of these questions. By visualizing protein-protein interactions within a cell, it might be possible to disentangle the complex network of interacting proteins and to gain an understanding of how the activity of proteins in the complex machinery of a cell is regulated by interacting proteins.

To conduct reliable measurements of the FRET efficiency between interacting proteins, however, not only a sophisticated setup but also bright and stable fluorescent labels are essential. The latter factor becomes increasingly important in experiments, where protein-protein interactions are traced over longer observation periods. Nowadays, a remarkable set of fluorescent proteins covering the entire visible spectrum is available.[12] From this collection, donor and acceptor fluorophores have to be chosen such that the emission spectrum of the donor and the absorption spectrum of the acceptor overlap to a certain extent, which is a prerequisite for FRET to occur. At the same time, the overlap between the donor and acceptor emission spectra should be as low as possible to minimize the cross-talk between donor and acceptor detection channels. These requirements narrow the choice of suitable fluorescent donor-acceptor pairs. Among them, the enhanced cyan fluorescent protein (ECFP) and the enhanced yellow fluorescent protein (EYFP) are very popular.[13,14] For intensity-based FRET measurements, ECFP and EYFP can be easily excited with a mercury lamp and appropriate filter sets or with the 458 nm and 514 nm line of an Argon laser. With a titanium:sapphire laser, ECFP can be excited by two-photon excitation, or the second harmonic of the laser beam can be used for one-photon excitation. The high repetition rate and the short pulse width (100 to 200 fs) of this laser makes it an excellent excitation source for lifetime-based FRET measurements as well.

In this paper, we show that FRET measurements involving fluorescent proteins need to be evaluated carefully, especially when ECFP is used as a donor fluorophore, since photobleaching and/or photoconversion can bias the results considerably. We studied these effects with a streak camera system that was connected to one of the detection channels of our confocal microscope. This system allowed us to record the fluorescence decays in a spectrally resolved manner.[15] To follow up changes in the emission properties of the fluorescent proteins during the course of the experiment, data were recorded in the so-called dynamic photon counting (dpc) mode. These data can be used for an offline analysis of the photon counting streak images as a function of irradiation time. Changes in both the spectra and the fluorescence decay of ECFP, which might occur upon irradiation, can be detected in this way. The results obtained for ECFP are compared with Cerulean, an ECFP variant that has been recently introduced.[16]

2 Methods

2.1 *DNA Vector Preparation, Transfection, and Cell Culture*

The plasmid encoding for ECFP (pECFP-C1) was obtained from Clontech (Clontech, Mountain View, California). pCerulean-C1 was designed by mutating pECFP-C1 at the following residues: S72A, Y145A, and H148D, according to Rizzo et al.[16] The plasmid encoding the EYFP-Cerulean hybrid protein was constructed as described earlier,[11] and the plasmid encoding the EYFP-ECFP hybrid protein was created in the same way. Restriction and sequencing analysis confirmed the correctness of both fusion constructs.

HEK293 cells were transfected using the conventional calcium phosphate precipitation technique and grown on coverslips. For confocal imaging and lifetime measurements, the coverslips were transferred to a microscope chamber that was superfused with phosphate buffered saline solution (PBS) containing (in mmol l^{-1}): NaCl 137, KCl 2.7, Na_2HPO_4 6.5, KH_2PO_4 1.5, pH 7.4.

2.2 *Isolation of Fluorescent Proteins*

Fluorescent proteins were expressed as soluble N-terminal hexa-His-tag fusions under control of an isopropyl-β-D-1-thiogalactopyranoside (IPTG) inducible promoter (pET16b vector) in *E. coli* BL21 (DE3). After cell lysis by ultrasonication, proteins were purified by metal chelate affinity chromatography (His-trap HP, Amersham), eluted with 250 mM imidazole, and dialyzed against a sodium phosphate buffer (50 mM NaH_2PO_4, 300 mM NaCl, pH 7.4) and diluted to a final concentration of 20 μM.

To investigate the effects of irradiation on the isolated proteins, the diluted protein solution was filled into capillaries with an inner diameter of 150 μm (Hilgenberg, Malsfeld, Germany). The droplets were small enough so that they could be scanned completely by our laser scanning microscope (LSM). To prevent evaporation during the course of the experiment, the capillaries were sealed with modeling clay.

2.3 *Experimental Setup*

A scheme of the setup used in this study is shown in Fig. 1(a). It consists of a laser scanning microscope (LSM-510, Carl Zeiss GmbH, Jena, Germany), a polychromator (250is, Chromex Inc., Albuquerque, New Mexico), and a streak camera (C5680 with a M5677 sweep unit, Hamamatsu Photonics Deutschland GmbH, Herrsching, Germany). The sample was excited by ultrashort light pulses that were generated by a mode-locked Titanium:Sapphire laser (Mira 900, Coherent GmbH, Dieburg, Germany) pumped by a 5 W, continuous-wave, frequency-doubled $Nd:YVO_4$ laser (5 W Verdi, Coherent). For measurements in cells, a pulse picker (Model 9200, Coherent) was used to decrease the frequency of the laser pulses to 2 MHz, the maximum repetition rate of the single-sweep unit of our streak camera. Isolated fluorescent proteins in capillaries were, however, exposed to the full repetition rate of the Titanium:Sapphire laser (78 MHz), while streak images were still acquired with a repetition rate of 2 MHz. In this way, we could follow up the effects of irradiation in a reasonable period of time despite the relatively large volume of the solution in the capillaries.

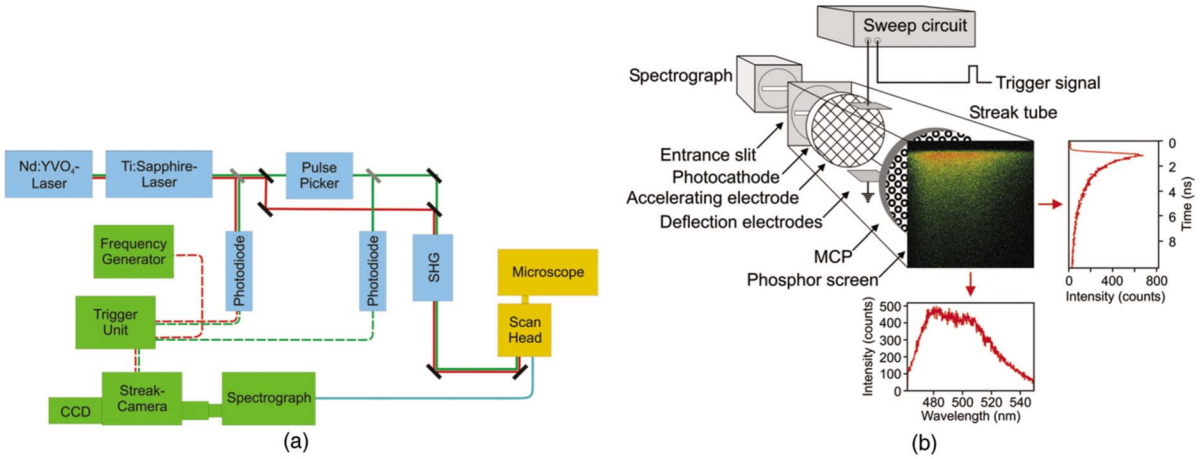

Fig. 1 (a) Setup: A Titanium:Sapphire laser that is pumped by a 5-W, frequency-doubled Nd:YVO_4 laser is used as pulsed excitation source. For experiments in cells (green lines), the repetition rate is decreased by a pulse picker to the maximal repetition rate (2 MHz) of the streak camera. For experiments in capillaries, the pulse picker is bypassed (red lines), and the sample is exposed to the full repetition rate of the Titanium:Sapphire laser. The second harmonic is generated by a BBO crystal and directed into the scan head of the laser scanning microscope. Emitted fluorescence light is collected by the water immersion objective, fed back through the scan head, and guided to one of the confocal channels. Here, the emitted light is coupled into an optical fiber and directed to a polychromator, where it is dispersed along the horizontal axis according to its wavelength. The dispersed spectrum is focused onto the entrance slit of the streak camera. (b) Operating principle of a streak camera: The light pulse to be measured is focused onto the photocathode of the streak tube, where photons are converted to electrons. The photoelectrons are accelerated by the accelerating electrode, pass through a pair of deflection plates, are multiplied in a micro-channel plate (MCP), and hit the phosphor screen of the streak tube, where they are converted to an optical image, the so-called streak image. At the instant the photoelectrons pass through the deflection electrodes, a voltage ramp is applied so that the electrons are swept from top to bottom. Electrons generated at earlier times arrive at the phosphor screen in a position close to the top of the screen, while those electrons that are generated at later times arrive at a position close to the bottom of the screen. Hence, the time at which a photon left the sample can be determined by the vertical position of the photoelectron in the streak image. The horizontal position of the photoelectron depends on the wavelength of the incident light pulse, since a spectrograph was used to focus the spectrum onto the photocathode. The streak image is read out by a CCD camera and transferred to a computer. From the streak image, the fluorescence spectrum can be obtained by summing up fluorescence intensities along the time axis (vertical axis) and plotting the resulting intensities versus the wavelength (horizontal axis). Accordingly, the fluorescence decay curve can be obtained by summing the fluorescence intensities in the wavelength region of interest and plotting the resulting intensities versus the time axis. (Color online only.) [Figure reprinted with permission from *Nature Biotechnology* (Ref. 15).]

The second harmonic (430 nm) of the pulse-picked or unmodified laser beam was generated by a β-barium borate (BBO) crystal. The beam was directed to the scan head of the confocal microscope. Cells were imaged with a 40× C-Apochromat water immersion objective (NA 1.20, Zeiss); capillaries were imaged with a 10× C-Apochromat water immersion objective (NA 0.45, Zeiss).

To measure the laser power in the focal plane, the diffuser and the sensor cell of a commercial power meter head (FieldMaster with LM2 head, Coherent) were removed and attached to a coverslip, which could be mounted in the same type of chamber we used for the confocal measurements of living cells. The active area of the sensor was large enough to collect all the light exiting the pupil of the objective. Comparison with a calibrated power meter showed that the power measurement with the modified power head was accurate.

For experiments in cells, the intensity of the laser beam (2 MHz) was attenuated by a neutral density filter so that the power in the focal plane was 1.0 μW. This beam was used to scan the sample continuously. The pixel dwell time was 6.4 μs. These settings correspond to settings that are used for fluorescence lifetime imaging experiments. For experiments in capillaries, the intensity of the laser beam (78 MHz) was adjusted with the neutral density filter so that the power in the focal plane was 100 μW. The region of interest (ROI) that was chosen for bleaching had a height of 10 pixels (18 μm) and a length that was equal to the full width of an image (512 pixel, 921.4 μm). The ROI was kept constant in all experiments and always positioned in the middle of the capillary so that all experiments are comparable to each other. The droplets were small enough so that the full length of the droplet was always scanned and exposed to the Titanium:Sapphire laser beam, which excludes the possibility that the measurement was biased by axial diffusion of ECFP or Cerulean from unexposed parts of the capillaries [Fig. 3(a)]. The scanning speed was adjusted such that the pixel dwell time was 6.4 μs.

In both *in vivo* and *in vitro* experiments, the fluorescence emitted by the sample was collected by the water immersion objective, fed back through the scan head, and guided to one of the confocal channels. Here, the emitted light was coupled into an optical fiber and directed to a polychromator. The polychromator spread the incident light along the horizontal axis and focused it on the entrance slit of the streak camera. The operation principle of the streak camera is explained in more detail in Fig. 1(b).[15,17] In brief, incoming photons hit the photocathode, where they are converted to photoelectrons. The photoelectrons are accelerated by the accelerating electrode, pass through a pair of deflection plates, are multiplied in a multichannel plate (MCP) and hit a phosphor screen, where they are reconverted to an optical image, the so-called streak image. At the instant the photoelectrons pass through the deflection electrodes, a voltage ramp is applied so that the

electrons are "swept" from top to bottom. Electrons leaving the photocathode at earlier times arrive at the phosphor screen in a position close to the top, whereas those electrons that leave the photocathode at a later time arrive at a position closer to the bottom. Thus, the vertical position of a spot depends on the time at which the photoelectron has left the photocathode; the horizontal position depends on the wavelength of the incident photon, because a spectrograph was used to focus the spectrum onto the streak-camera entrance slit. The streak images are read out by a CCD camera and transferred in 111-ms intervals to a computer, where they are accumulated to yield the final photon counting streak images. In parallel, detected photons were recorded in dynamic photon counting (dpc) files, in which photons are saved with a time tag allowing for a detailed time-dependent analysis of both the spectrum and the fluorescence decays during the measurement period.

2.4 *Data Analysis*

To visualize and evaluate changes, which occur during irradiation, streak images were reconstructed in 5-min time intervals from the dpc files. From these streak images, fluorescence spectra and fluorescence decays were extracted, as shown in Fig. 1(b). Fluorescence decays were evaluated using the "iterative reconvolution method" and a modified Gaussian-Newtonian algorithm to approximate the parameters of a mono- or biexponential model. All steps of the analysis were performed using our own software, which was developed using MATLAB (MathWorks, Natick, Massachusetts). The goodness of the fit was judged by the value of the reduced χ_v^2.

Since, in most cases, a biexponential model had to be chosen to fit the data adequately, we decided to fit all data to a biexponential model to better quantify the acceleration of the fluorescence decay upon irradiation. To facilitate the direct comparison of the data, amplitude-weighted mean lifetimes (τ_m) were calculated from the parameters of the biexponential fit according to:

$$\tau_m = A_f \tau_f + A_s \tau_s, \tag{1}$$

where A_f and A_s are the relative amplitudes of the fast (τ_f) and slow (τ_s) lifetime component, respectively.[18] τ_m is equal to the area under the (normalized) fluorescence decay curve. It can also be regarded as a measure for the intensity one would have observed in an intensity-based FRET experiment.

The FRET efficiency is defined as the fraction of energy absorbed by the donor that is transferred to the acceptor. It is given by the ratio between the energy transfer rate and the total fluorescence decay rate of the donor. It can be calculated by comparing the fluorescence intensity (I_{DA}) or fluorescence lifetime (τ_{DA}) of the donor in presence of an acceptor with the fluorescence intensity (I_D) or fluorescence lifetime (τ_D) of the donor in absence of an acceptor:

$$E = 1 - \frac{I_{DA}}{I_D}, \tag{2}$$

$$E = 1 - \frac{\tau_{DA}}{\tau_D}. \tag{3}$$

In an ideal scenario, the donor fluorophore employed in FRET experiments exhibits a monoexponential fluorescence decay. Then, in the presence of an interaction partner labeled with an appropriate acceptor fluorophore, one would observe a biexponential fluorescence decay, in which the fast lifetime component (τ_f) could be attributed to the fraction of interacting donor molecules whose lifetime is quenched by FRET. The slow lifetime component (τ_s) would be caused by free, noninteracting donor molecules and should be close to the control values obtained in absence of the acceptor.[11,19] In this case, the FRET efficiency of a donor-acceptor pair would have been calculated by relating the fast lifetime component of the biexponential fit to the donor fluorescence lifetime obtained in control measurements.

In this study, however, we show that fluorescence lifetimes of ECFP and Cerulean decrease upon prolonged irradiation and exhibit a pronounced biexponential fluorescence decay. To better describe the fluorescence decay and quantify the area under the decay curve, we used the amplitude weighted mean lifetimes (τ_m) for calculating the "apparent" FRET efficiency. This approach is justified in so far as we do not investigate a mixed system of interacting and noninteracting donor molecules: Cells express either the donor molecules alone or hybrid proteins, in which donor and acceptor are covalently linked to each other. Thus, only one population of donor molecules exists. The one and only aim of this approach is to demonstrate the errors one can make when the observed decrease in the fluorescence lifetime is erroneously attributed to FRET.

3 Results

3.1 *Streak Camera Measurements of ECFP and Cerulean*

To investigate the changes in the photophysical properties of ECFP and Cerulean induced by irradiation, we expressed ECFP and Cerulean in HEK293 cells and scanned the cells continuously on the stage of a confocal microscope with the pulse-picked (2 MHz) and frequency-doubled laser beam (λ =430 nm). The intensity was attenuated by a neutral density filter so that the power in the focal plane was 1.0 μW. These settings correspond to settings that are used for fluorescence lifetime imaging experiments. Figure 2(b) shows streak images of ECFP (upper panel) and Cerulean (lower panel) that have been obtained during an acquisition period of 25 min. In addition to the streak images, so-called dynamic photon counting (dpc) files were recorded, in which each detected photon is saved with a time tag along with its wavelength and time coordinates. This information can be used to follow up in an offline analysis the total number of emitted photons as a function of time, or to recover streak images, fluorescence spectra, or fluorescence decays in any time intervals of interest. Figures 2(c) and 2(e) show an overlay of spectra and fluorescence decays, respectively, that have been reconstructed from the dpc data in 5-min intervals. The overlay of the fluorescence spectra of ECFP [Fig. 2(c), upper panel] shows that the amplitude of the fluorescence spectra decreased during the course of the experiment. Superposition of the normalized fluorescence decays [Fig. 2(e), upper panel] shows that the fluorescence decay also underwent changes during the course of the experiment. It was accelerated upon

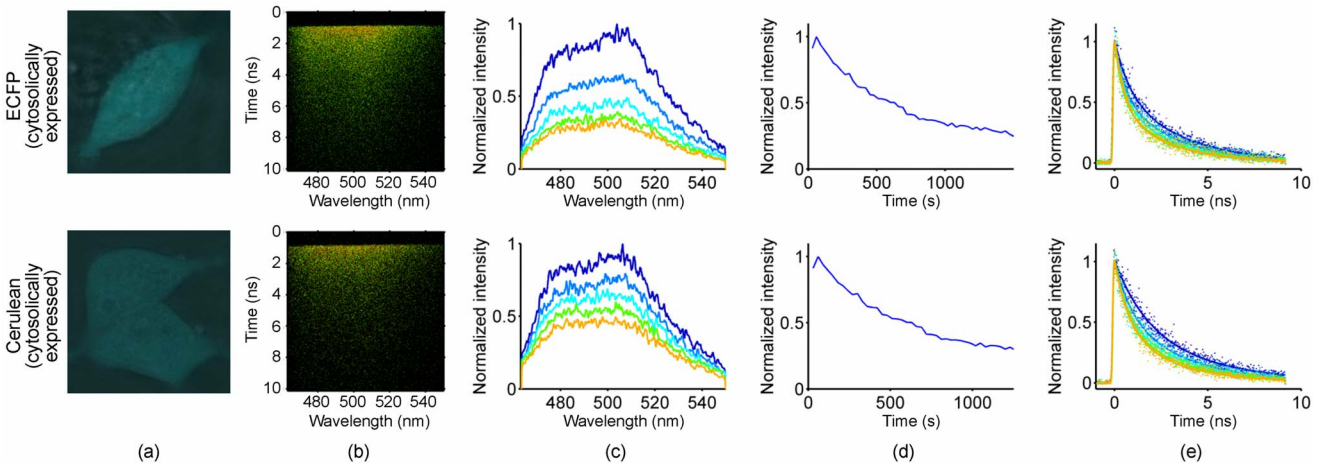

Fig. 2 Analysis of streak images obtained from HEK293 cells expressing ECFP and Cerulean. (a) Confocal image of HEK293 cells expressing ECFP (upper panel) and Cerulean (lower panel). (b) Streak images obtained from the cells shown in (a). Each dot in the streak image represents one photon that was detected during the measurement. The *x* coordinate is determined by its wavelength, and the *y* coordinate depends on the time after the excitation pulse. Counts per pixel are encoded by color ranging from black (no counts) through green and yellow to red (high count rate). (c) Fluorescence emission spectra of ECFP (upper panel) and Cerulean (lower panel) obtained in 5-min time intervals (from top to bottom: 0 to 5 min: dark blue; 5 to 10 min: light blue; 10 to 15 min: cyan; 15 to 20 min: green; 20 to 25 min: orange). The fluorescence emission spectra have been reconstructed from the respective dpc files. All spectra have been normalized with respect to the peak of the respective emission spectrum. (d) Time course of the fluorescence intensity of ECFP (upper panel) and Cerulean (lower panel) in the wavelength range from 465 nm to 495 nm. Counts in the wavelength range from 465 nm to 495 nm have been binned in 1-min intervals and normalized with respect to the highest count rate at the beginning of the recording. (e) Fit of the fluorescence decay curves of ECFP (upper panel) and Cerulean (lower panel) in the wavelength range from 465 to 495 nm obtained in 5-min time intervals (from top to bottom: 0 to 5 min: dark blue; 5 to 10 min: light blue; 10 to 15 min: cyan; 15 to 20 min: green; 20 to 25 min: orange). The fluorescence decay curves have been reconstructed from the respective dpc files. To facilitate comparison of the decay kinetics, all curves have been normalized with respect to their maximum. (Color online only.)

prolonged irradiation. In the example shown, the mean lifetime decreased by 19% from τ_m (5 min) = 2.29 ns to τ_m (10 min) = 1.85 ns and further down to τ_m (25 min) = 1.44 ns. In a series of eight experiments, the mean fluorescence lifetime decreased from $\overline{\tau_m}$ (5 min) = (2.33 ± 0.19) ns to $\overline{\tau_m}$ (25 min) = (1.28 ± 0.22) ns.

Cerulean (Fig. 2, lower row) showed a similar behavior, although the changes in the fluorescence spectra [Fig. 2(c), lower row] were not so pronounced as in the ECFP spectra. Also, the fluorescence decay curves were accelerated upon prolonged irradiation. In the example shown, the mean lifetime decreased by 22% from τ_m (5 min) = 2.96 ns to τ_m (10 min) = 2.32 ns and further down to τ_m (25 min) = 1.71 ns. In a series of nine experiments, the mean fluorescence lifetime decreased from $\overline{\tau_m}$ (5 min) = (2.66 ± 0.13) ns to $\overline{\tau_m}$ (25 min) = (1.52 ± 0.25) ns.

These results could be confirmed for ECFP and Cerulean that were expressed as *N*-terminal His-tag fusions in *E. coli* and purified by nickel affinity chromatography. The purified proteins were diluted with PBS to a final concentration of 20 μM. A small aliquot of this solution was filled into a capillary with an inner diameter of 150 μm and imaged on the stage of our confocal microscope. To better observe the effects of irradiation despite the bigger volume, the sample was exposed to the full repetition rate of the Titanium:Sapphire laser. The intensity was adjusted so that the power in the focal plane was 100 μW. The pixel dwell time was set to 6.4 μs. Again, ECFP exhibited a decrease in both fluorescence intensity and fluorescence lifetime upon irradiation (Fig. 3, upper row). Here, the mean fluorescence lifetime decreased by 23% from τ_m (5 min) = 2.20 ns to τ_m (30 min) = 1.70 ns after 30-min exposure. In a series of eight experiments, the mean fluorescence lifetime decreased from $\overline{\tau_m}$ (5 min) = (2.19 ± 0.11) ns to $\overline{\tau_m}$ (30 min) = (1.64 ± 0.06) ns.

Under the same conditions, Cerulean (Fig. 3, lower row) exhibits similar changes. In the example shown, the mean fluorescence lifetime changed by 23% from τ_m (5 min) = 2.89 ns at the beginning to τ_m (30 min) = 2.23 ns at the end of the experiment. In a series of nine experiments, the mean fluorescence lifetime decreased from $\overline{\tau_m}$ (5 min) = (2.86 ± 0.09) ns to $\overline{\tau_m}$ (30 min) = (2.19 ± 0.18) ns.

3.2 *Streak Camera Measurements of Hybrid Proteins*

The fluorescence decays measured in cells or in the capillary show that ECFP and Cerulean are not ideal donor molecules in experiments, where FRET efficiency is monitored over a longer observation period: In intensity-based estimates of the FRET efficiency, the decrease in fluorescence intensity would be erroneously attributed to FRET. Likewise, the decrease in the ECFP lifetime might invalidate measurements of the donor fluorescence lifetime. To demonstrate how an estimate of FRET can be biased by prolonged irradiation, we constructed an EYFP–Cerulean hybrid protein, in which the donor fluorophore (e.g., ECFP or Cerulean) and the acceptor fluorophore (e.g., EYFP) were closely linked by a short sequence of 10 amino acids (see Sec. 2.1). Figure 4(b) shows the streak images obtained from Hek293 cells expressing these hybrid proteins. Comparison with the respective streak images from cells expressing only the donor molecules [Fig. 2(b)] shows that the donor (ECFP or Cerulean) fluorescence signal in the wavelength range between 465 and 495 nm is decreased, whereas the acceptor (EYFP) fluorescence between 510 and

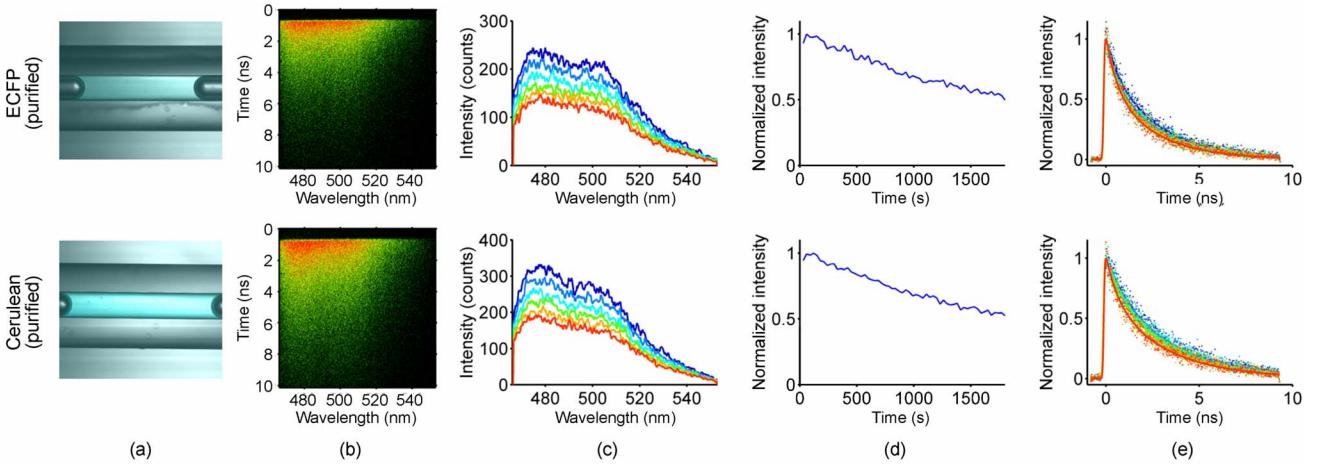

Fig. 3 Analysis of streak images obtained from isolated ECFP and Cerulean. (a) Confocal image of capillaries filled with purified ECFP (upper panel) and Cerulean solution (lower panel). (b) Streak images obtained from the capillaries shown in (a). (c) Fluorescence emission spectra of ECFP (upper panel) and Cerulean (lower panel) obtained in 5-min time intervals (from top to bottom: 0 to 5 min: dark blue; 5 to 10 min: light blue; 10 to 15 min: cyan; 15 to 20 min green; 20 to 25 min: orange; 25 to 30 min: red). (d) Time course of the fluorescence intensity of ECFP (upper panel) and Cerulean (lower panel) in the wavelength range from 465 to 495 nm. (e) Fluorescence decay curves of ECFP (upper panel) and Cerulean (lower panel) in the wavelength range from 465 nm to 495 nm obtained in 5-min time intervals. Colors are assigned as described earlier. All data have been processed as described in Fig. 2. (Color online only.)

540 nm is increased. This is also demonstrated by the spectrum [Fig. 4(c)] and the fluorescence decays [Fig. 4(e)] that were reconstructed from the respective dpc files. Compared to the spectrum of ECFP or Cerulean, the emission peak of the fluorescence spectrum of the EYFP–ECFP and the EYFP–Cerulean hybrid protein was shifted toward acceptor emission wavelengths, and the fluorescence decay of the ECFP and Cerulean moiety in the hybrid protein was accelerated. Compared to ECFP, whose lifetime was determined to be (2.33 ± 0.19) ns in living cells, the fluorescence lifetime of the EYFP–CFP hybrid protein was accelerated to τ_m (5 min) = 1.59 ns. Upon irradiation, the donor fluorescence lifetime decreased further to τ_m (25 min) = 0.98 ns. In a series of seven experiments, the mean fluorescence lifetime decreased from $\overline{\tau_m}$ (5 min) = (1.45 ± 0.11) ns to

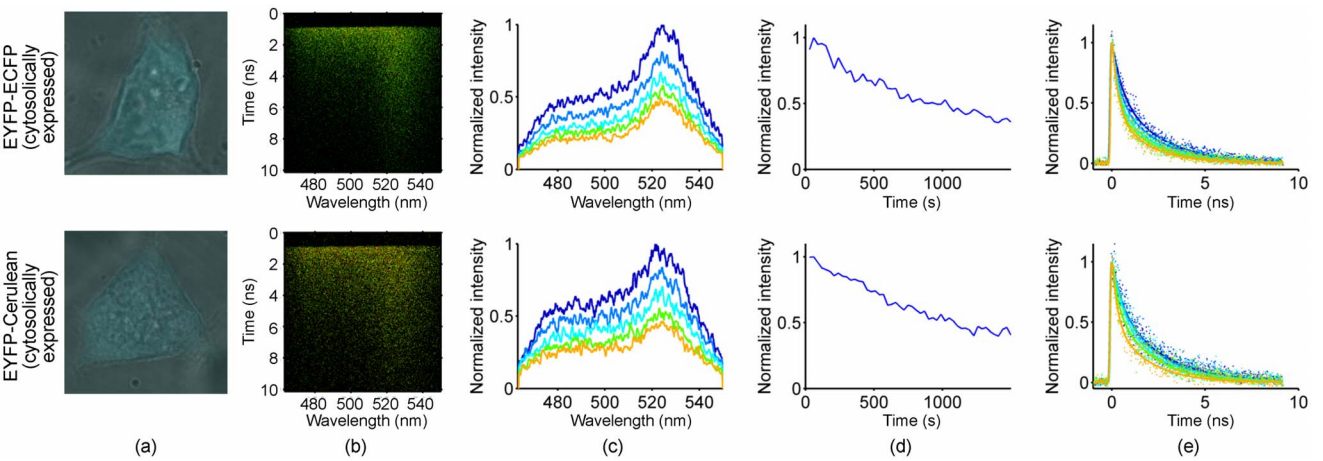

Fig. 4 Analysis of streak images obtained from HEK293 cells expressing the EYFP-ECFP and EYFP-Cerulean hybrid protein. (a) Confocal image of HEK293 cells expressing the EYFP-ECFP hybrid protein (upper panel) and the EYFP-Cerulean hybrid protein (lower panel). (b) Streak images obtained from the cells shown in (a). The comparison with the streak images of ECFP and Cerulean [Fig. 2(b)] shows that the fluorescence signal in the wavelength range between 465 and 495 nm is decreased, whereas the acceptor (EYFP) fluorescence in the wavelength range between 510 and 540 nm is increased considerably. (c) Fluorescence emission spectra of the EYFP-ECFP hybrid (upper panel) and the EYFP-Cerulean hybrid protein (lower panel) obtained in 5-min time intervals. Compared to the fluorescence spectra of HEK293 cells expressing ECFP or Cerulean [Fig. 2(c)] alone, the peak of the fluorescence spectrum is shifted toward acceptor emission wavelengths. (d) Time course of the fluorescence intensity of the EYFP-ECFP hybrid protein (upper panel) and the EYFP-Cerulean hybrid protein (lower panel) in the wavelength range from 465 to 495 nm. (e) Fluorescence decay curves of the EYFP-ECFP hybrid protein (upper panel) and the EYFP-Cerulean hybrid protein (lower panel) obtained in 5-min time intervals in the wavelength range from 465 to 495 nm. Compared to the fluorescence decays observed in HEK293 cells expressing ECFP or Cerulean [Fig. 2(e)], the fluorescence decay is accelerated. All data have been processed as described in Fig. 2. Colors are assigned accordingly. (Color online only.)

$\overline{\tau_m}$ (25 min) = (0.98 ± 0.08) ns. When it is assumed that donor and acceptor fluorophores are separated by a single distance, a FRET efficiency of 37% can be calculated with Eq. (3) from the initial value. During the course of the experiment, however, the lifetime decreased to τ_m (25 min) = 0.98 ns. Based on the latter value, a FRET efficiency of 58% would be calculated, which is beyond the maximal FRET efficiency that should be expected for an ECFP–EYFP FRET pair: GFP and its variants consist of an 11-stranded β-barrel, which has the shape of a cylinder with a length of 4.2 nm and a diameter of 2.4 nm.[14,20] Since the fluorophore is located almost in the geometric center of the cylinder,[14,20] the minimal distance between the fluorophores that is physically possible is about 5 nm. This is close to the Förster distance of 4.9 nm for the ECFP and EYFP pair.[21] Thus, with a stoichiometry of 1:1 between donor and acceptor molecules, FRET efficiencies above 50% should not be observed.

Similar results are observed for the analog hybrid-protein containing the Cerulean fluorophore: Compared to Cerulean alone, whose lifetime was determined to be (2.66 ± 0.13) ns in living cells, the fluorescence lifetime of the EYFP–Cerulean hybrid protein was decreased to τ_m (5 min) = 1.75 ns and τ_m (25 min) = 0.95 ns. In a series of eight experiments, fluorescence lifetimes decreased from $\overline{\tau_m}$ (5 min) = (1.71 ± 0.07) ns to $\overline{\tau_m}$ (25 min) = (1.01 ± 0.09) ns. The first value would correspond to a FRET efficiency of 35%, which is almost identical to the FRET efficiency calculated in the case of the EYFP–ECFP hybrid protein. After irradiation, a FRET efficiency of 62% would have been calculated.

4 Discussion

When and where proteins associate with each other in living cells are key questions in many biological research projects. One way to address these questions is to measure the extent of FRET between proteins that have been labeled with appropriate donor and acceptor fluorophores. Many methods have been published to estimate the extent of FRET. Among them, fluorescence lifetime imaging (FLIM) microscopy is considered to be one of the most reliable methods for FRET measurements in living cells, since fluorescence lifetimes are insensitive to variations in the concentration of the fluorophores, fluctuations in the power of the illumination source, and alterations in the optical path.[22] But the experiments presented in this paper demonstrate that special care has to be taken when ECFP and Cerulean are used as donor fluorophores. It has been already shown that fluorescence intensities of ECFP, Cerulean, and other VFPs[23,24] decrease upon one- or two-photon excitation. Here, we show also that the fluorescence lifetimes of ECFP and Cerulean decrease upon irradiation, which might seriously impede the interpretation of lifetime-based FRET experiments using ECFP or Cerulean as donor molecules. If these effects are not taken into account, the decrease in donor fluorescence lifetime might be erroneously attributed to FRET, resulting in overestimated FRET efficiencies: During the course of our experiment, ECFP bleached to an extent of more than 50%; during this period, the lifetime decreased from 2.33 ns to 1.28 ns. The lifetime after irradiation was close to a value (1.45 ns) we observed initially for the hybrid protein. Being unaware of this effect, one would have misinterpreted the decrease in donor fluorescence lifetime as FRET. The same applies to Cerulean, which also bleached to an extent of more than 50% during the course of the experiment and whose lifetime decreased from 2.66 ns to 1.52 ns. These results could be confirmed for the isolated proteins: Upon irradiation, the fluorescence lifetimes of both ECFP and Cerulean decreased.

In principle, several processes can contribute to such a decrease in fluorescence lifetime:

- *Photobleaching*: If ECFP and Cerulean were a mixture of two isomers of different lifetimes and if the component with the longer fluorescence lifetime photobleached more rapidly, then the overall fluorescence lifetime of the mixture of both isomers would decrease upon irradiation.
- *Photoconversion*: Irradiation of ECFP and Cerulean could induce a photochemical reaction of the chromophore that yielded an isomer with a shorter fluorescence lifetime.

From the present data, it is difficult to distinguish between both cases. At first glance, the first mechanism appears to be supported by the crystal structure of ECFP, which shows that indeed two isomeric forms of ECFP exist.[25] According to the crystal structure, the overall topology of ECFP is mainly identical to that of the 11-stranded GFP β-barrel, with the autocatalytically formed chromophore positioned (in a single conformation) within the central helix. Structural differences arise from the residues Tyrl45 and Hisl48 that are oriented toward the chromophore in GFP, whereas in one of the ECFP conformations, either the Tyrl45 (B′ conformation) or the His148 side-chain (A′ conformation) is moved toward the outside and exposed to the solvent. Although it is tempting to speculate that these structural properties might give rise to the fluorescent properties, proof for such a correlation does not exist. In contrast, ^{19}F NMR studies indicate that the conformations interconvert on a millisecond time scale.[25,26] In our study, however, we show that the mean fluorescence lifetime decreases and remains shortened over the entire measurement period, which indicates that the isomers do not interconvert. If the isomers interconverted on a millisecond time scale, a decrease of the fluorescence lifetime should not be observed. Thus, in our eyes, it is unlikely that the two structural arrangements of ECFP that are identified by the crystal structure are the basis for the two lifetime components of ECFP we observed in our experiments.

In Cerulean, the mutation H148D was introduced to stabilize the solvent exposure of this residue (by substituting the imidazole with a carboxyl group), but surprisingly, the structural arrangement of Cerulean in this region follows closely the structure of the ECFP B′ structure.[27] The hydrophilic carboxyl group of H148D points toward the interior, whereas the hydrophobic methyl group of Y145A is exposed to the solvent. Contrary to ECFP, the indole group of Cerulean adopts a cis configuration with respect to the imidazoline ring chromophore itself. The x-ray structure of Cerulean shows only a single conformation of the chromophore and the surrounding residues. Accordingly, only one fluorescence lifetime should be observed, which is (almost) the case for the unexposed sample. However, our results show that upon irradiation, a second isomer predominates. Relating these structural details to the fluorescence properties is, however, difficult. It appears that the protein main chain plays an important role in stabilizing the chromophore structure in both the trans- or cis-

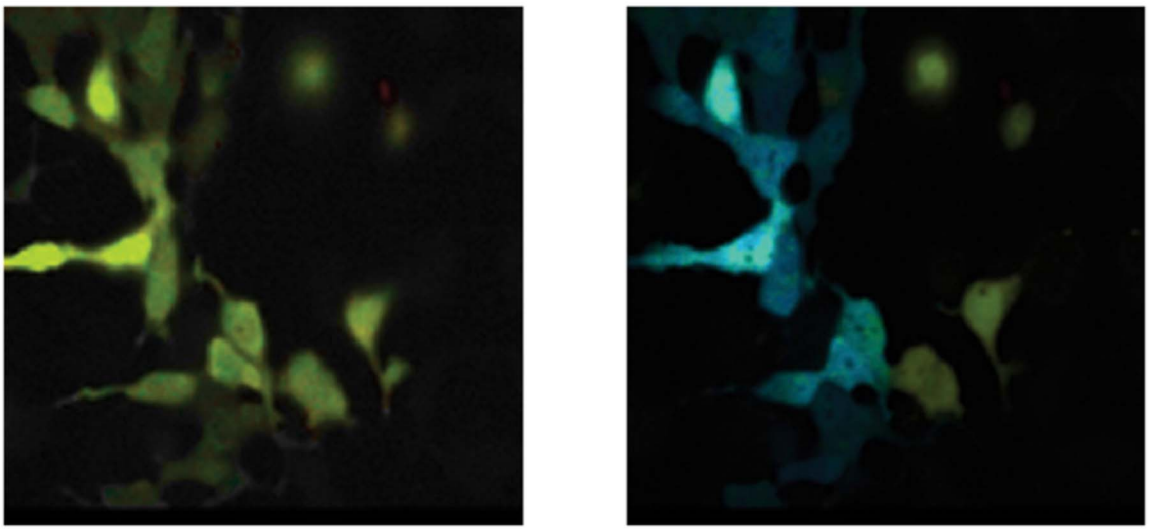

Fig. 5 Fluorescence lifetime images obtained from HEK293 cells expressing the EYFP-ECFP hybrid protein in the cytosol. (a) Fluorescence lifetime image of HEK293 cells expressing the EYFP-ECFP hybrid protein cytosolically. Fluorescence lifetime data have been acquired by using the TCSPC technique. A biexponential function has been fitted to the fluorescence decay curves recorded in each pixel. Mean fluorescence lifetimes are encoded by color ranging from red (1.0 ns) to blue (3.0 ns). (b) Fluorescence lifetime recorded after acceptor photobleaching. The acceptor has been bleached with the Ar 514-nm line in the left part of the scanning field. Fluorescence lifetimes in this part of the scan area recovered to the control values. This experiment proves that the decrease in the fluorescence lifetime recorded before acceptor photobleaching is due only to FRET and not to artifacts. (Color online only.)

configuration and might be an important factor influencing the fluorescence lifetime of ECFP and Cerulean, respectively. It might be that subtle structural changes, which cannot be resolved by the x-ray structure, have a dramatic impact on the fluorescence lifetime. On the other hand, the fact that the fluorescence lifetimes are changed irreversibly (at least on the time scale of our experiments) indicates that the energy barrier between the isomers must be at least high enough that the isomers do not interconvert at room temperature. In this light, a photoinduced reaction (e.g., photoconversion) might appear as a good explanation of the decrease of the fluorescence lifetime. But most likely both mechanisms, photobleaching and photoconversion, occur simultaneously. No matter what mechanism is involved, the fact that the shape of the fluorescence emission spectra does not change noticeably during exposure indicates that the isoforms involved have similar emission spectra.

In our experiments, ECFP and Cerulean were exposed to the same laser power. Under these conditions, ECFP and Cerulean show a considerable decrease in both the fluorescence intensity and the fluorescence lifetime. But when comparing the data, one has to keep in mind that compared to ECFP, Cerulean has a higher extinction coefficient ($43{,}000\ M^{-1}\,cm^{-1}$ versus $29{,}000\ M^{-1}\,cm^{-1}$) and a higher quantum yield (0.62 versus 0.37). Thus, with respect to the number of photons emitted by the sample, Cerulean makes up a much better tag for both intensity- and lifetime-based FRET measurements. This, however, does not mean that it is not possible to get reasonable results with ECFP as a donor fluorophore. The comparison of the FRET efficiencies obtained from the EYFP–ECFP hybrid protein after 5 min of irradiation with the homolog Cerulean protein shows also that experiments based on ECFP lifetime measurements can yield good results. One has only to make sure that excitation time and excitation power are kept low. In the setting of a confocal microscope, this applies not only for the laser, but also for the mercury lamp. Tramier et al.[28] have nicely shown also that illumination with a mercury lamp for less than a minute can decrease the ECFP lifetime considerably. Thus, even during the screening for transfected cells, fluorescence lifetimes can be artificially decreased. This can explain the variability observed in ECFP lifetime measurements and emphasizes the need for additional controls to verify that observed decreases in donor fluorescence lifetime are due only to FRET and not to photoconversion. Such an additional control can be achieved by spectrally resolved fluorescence lifetime measurements in a streak camera or a multiwavelength time-correlated single photon counting (TCSPC) setup, in which both the donor and the acceptor fluorescence decay are recorded simultaneously. With these techniques, it is possible to verify that the observed decrease in donor fluorescence lifetime is matched by a corresponding increase of acceptor fluorescence, which at the same time excludes that the decrease in donor lifetime is caused by other quenching processes, photobleaching, and/or photoconversion. Another useful control, which can even be performed in a conventional TCSPC setup, would be to photobleach the acceptor after the experiment, as it is shown in the example presented in Fig. 5. If a decrease in donor fluorescence lifetime is exclusively due to FRET, then the donor lifetime must recover to control values after photobleaching of the acceptor.

Acknowledgments

We thank Karin Schoknecht for excellent technical assistance and Gerhard Rousseau for helpful hints in modifying our streak camera setup.

References

1. O. Shimomura, F. H. Johnson, and Y. Saiga, "Extraction, purification, and properties of aequorin, a bioluminescent protein from the luminous hydromedusa, *Aequoria*," *J. Cell. Comp. Physiol.* **59**(3), 223–239 (1962).
2. D. C. Prasher, V. K. Eckenrode, W. W. Ward, F. G. Prendergast, and M. J. Cormier, "Primary structure of the *Aequorea victoria* green-fluorescent protein," *Gene* **111**(2), 229–233 (1992).
3. M. Chalfie, Y. Tu, G. Euskirchen, W. W. Ward, and D. C. Prasher, "Green fluorescent protein as a marker for gene expression," *Science* **263**(5148), 802–805 (1994).
4. S. Inouye and F. I. Tsuji, "*Aequorea* green fluorescent protein: expression of the gene and fluorescence characteristics of the recombinant protein," *FEBS Lett.* **341**(2–3), 277–280 (1994).
5. R. Y. Tsien, "The green fluorescent protein," *Annu. Rev. Biochem.* **67**, 509–544 (1998).
6. R. M. Clegg, "Fluorescence resonance energy transfer," in *Fluorescence Imaging Spectroscopy and Microscopy*, X. F. Wang and B. Herman, Eds., Chemical Analysis Series, Vol. 137, pp. 179–251, John Wiley & Sons, New York (1996).
7. G. W. Gordon, G. Berry, X. H. Liang, B. Levine, and B. Herman, "Quantitative fluorescence resonance energy transfer measurements using fluorescence microscopy," *Biophys. J.* **74**, 2702–2713 (1998).
8. Y. Chen, J. P. Mauldin, R. N. Day, and A. Periasamy, "Characterization of spectral FRET imaging microscopy for monitoring nuclear protein interactions," *J. Microsc.* **228**(2), 139–152 (2007).
9. A. Periasamy, "Fluorescence resonance energy transfer microscopy: a mini review," *J. Biomed. Opt.* **6**(3), 287–291 (2001).
10. A. Periasamy and R. N. Day, *Molecular Imaging: FRET Microscopy and Spectroscopy: Methods in Physiology*, Oxford University Press, Oxford (2005).
11. C. Biskup, T. Zimmer, L. Kelbauskas, B. Hoffmann, N. Klöcker, W. Becker, A. Bergmann, and K. Benndorf, "Multi-dimensional fluorescence lifetime and FRET measurements," *Microsc. Res. Tech.* **70**(5), 442–451 (2007).
12. N. C. Shaner, P. A. Steinbach, and R. Y. Tsien, "A guide to choosing fluorescent proteins," *Nat. Methods* **2**(12), 905–909 (2005).
13. R. Heim and R. Y. Tsien, "Engineering green fluorescent protein for improved brightness, longer wavelengths, and fluorescence resonance energy transfer," *Curr. Biol.* **6**(2), 178–182 (1996).
14. M. Ormö, A. B. Cubitt, K. Kallio, L. A. Gross, R. Y. Tsien, and S. J. Remington, "Crystal structure of the *Aequorea victoria* green fluorescent protein," *Science* **273**(5280), 1392–1395 (1996).
15. C. Biskup, T. Zimmer, and K. Benndorf, "FRET between cardiac Na^+ channel subunits measured with a confocal microscope and a streak camera," *Nat. Biotechnol.* **22**(2), 220–224 (2004).
16. M. A. Rizzo, G. H. Springer, B. Granada, and D. W. Piston, "An improved cyan fluorescent protein variant useful for FRET," *Nat. Biotechnol.* **22**(4), 445–449 (2004).
17. T. M. Nordlund, "Streak cameras for time-domain fluorescence," in *Topics in Fluorescence Spectroscopy, Volume 1: Techniques*, J. R. Lakowicz, Ed., pp. 183–260, Plenum Press, New York (1991).
18. J. R. Lakowicz, *Principles of Fluorescence Spectroscopy*, 3rd ed., Springer, Singapore (2006).
19. C. Biskup, L. Kelbauskas, T. Zimmer, K. Benndorf, A. Bergmann, W. Becker, J. P. Ruppersberg, C. Stockklausner, and N. Klöcker, "Interaction of PSD-95 with potassium channels visualized by fluorescence-lifetime-based resonance energy transfer imaging," *J. Biomed. Opt.* **9**(4), 753–759 (2004).
20. F. Yang, L. G. Moss, and G. N. Phillips, "The molecular structure of green fluorescent protein," *Nat. Biotechnol.* **14**(10), 1246–1251 (1996).
21. G. H. Patterson, D. W. Piston, and B. G. Barisas, "Förster distances between green fluorescent protein pairs," *Anal. Biochem.* **284**(2), 438–440 (2000).
22. K. Suhling, P., M. W. French, and D. Phillips, "Time-resolved fluorescence microscopy," *Photochem. Photobiol. Sci.* **4**(1), 13–22 (2005).
23. G. H. Patterson, S. M. Knobel, W. D. Sharif, S. R. Kain, and D. W. Piston, "Use of green fluorescent protein and its mutants in quantitative fluorescence microscopy," *Biophys. J.* **73**(5), 2782–2790 (1997).
24. T. S. Chen, S. Q. Zeng, Q. M. Luo, Z. H. Zhang, and W. Zhou, "High-order photobleaching of green fluorescent protein inside live cells in two-photon excitation microscopy," *Biochem. Biophys. Res. Commun.* **291**(5), 1272–1275 (2002).
25. J. H. Bae, M. Rubini, G. Jung, G. Wiegand, M. H. J. Seifert, M. K. Azim, J. S. Kim, A. Zumbusch, T. A. Holak, L. Moroder, R. Huber, and N. Budisa, "Expansion of the genetic code enables design of a novel 'gold' glass of green fluorescent proteins," *J. Mol. Biol.* **328**(5), 1071–1081 (2003).
26. M. H. J. Seifert, D. Ksiazek, M. K. Azim, P. Smialowski, N. Budisa, and T. A. Holak, "Slow exchange in the chromophore of a green fluorescent protein variant," *J. Am. Chem. Soc.* **124**(27), 7932–7942 (2002).
27. G. D. Malo, L. J. Pouwels, M. Wang, A. Weichsel, W. R. Montfort, M. A. Rizzo, D. W. Piston, and R. M. Wachter, "X-ray structure of Cerulean-GFP: a tryptophan-based chromophore useful for fluorescence lifetime imaging," *Biochem. J.* **46**(35), 9865–9873 (2007).
28. M. Tramier, M. Zahid, J. C. Mevel, M. J. Masse, and M. Coppey-Moisan, "Sensitivity of CFP/YFP and GFP/mCherry pairs to donor photobleaching on FRET determination by fluorescence lifetime imaging microscopy in living cells," *Microsc. Res. Tech.* **69**(11), 933–939 (2006).